Lab on a Chip

Accepted Manuscript

ROYAL SOCIETY OF CHEMISTRY

www.rsc.org/loc

Table of Contents Graphic

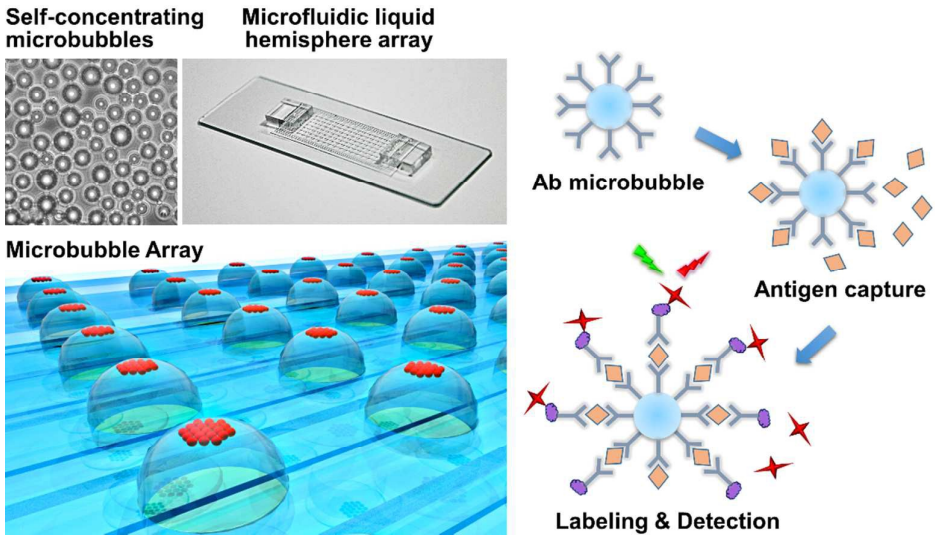

A self-concentrating buoyant glass microbubble material for enhancing the sensitivity of immunoassays.

Lab on a Chip

TECHNICAL INNOVATION

Self-concentrating buoyant glass microbubbles for high sensitivity immunoassays

Received 00th January 20xx,
Accepted 00th January 20xx

DOI: 10.1039/x0xx00000x

www.rsc.org/

Duane S. Juang[ab] and Chia-Hsien Hsu*[a]

Here, we report the novel application of a material with self-concentrating properties for enhancing the sensitivity of immunoassays. Termed as glass microbubbles, they are antibody functionalized buoyant hollow glass microspheres that simultaneously float and concentrate into a dense monolayer when dispensed in a liquid droplet. This self-concentrating charactaristic of microbubbles allow for autonomous signal localization, which translates to a higher sensitivity compared to other microparticle based immunoassays. We then demonstrated a "microbubble array" platform consisting of the glass microbubbles floating in a microfluidic liquid hemisphere array for performing multiplex immunoassays.

Immunoassays are one of the most widely used analytical methods in clinical diagnostics and biomedical laboratories. The traditional and most commonly used form of immunoassay is the Enzyme-linked immunosorbent assay (ELISA), which provides the advantage of high operational compatibility with conventional 96 well plates. However, the operation of ELISA requires larger amounts of samples and reagents, long incubation periods, and labor intensive repetitive pipetting, thus limiting its throughput without using a robotic machine. Therefore, there has been a growing interest in developing miniaturized platforms for immunoassays. A recently popular approach for developing miniaturized immunoassays are microparticle based platforms, which benefit from higher sensitivity and flexibility due to their faster binding kinetics, a much larger surface to volume ratio, and the simplicity and flexibility of off-chip batch surface modification[1, 2]. However, microparticles have an inherent nature of getting randomly dispersed in fluid, leading to signal detection difficulties because of (a) dispersion of signal as microparticles are difficult to concentrate in a small area for signal enhancement, (b) the requirement of a high magnification objective lens to capture the weak signal from small individual microparticles, and (c) laborious signal quantification as an individual selection is required for each small microparticle in a large field of vision. As opposed to letting microparticles randomly distribute in a solution, physically concentrating microparticles in a dense region can greatly improve the strength and quality of the assay signal during imaging[3, 4]. Previously, many particle concentrating methods have been developed in an attempt to address these problems, including mechanical trapping[4], dielectrophoretic trapping[5], optical trapping[6], and magnetic trapping[7]. However, these methods also add complexities and additional costs to the assay.

Here, we report a new class of microparticles, when combined with micro droplets can self-concentrate to enhance the sensitivity of immunoassays detection. Known as Glass microbubbles (3M Corp.), they are an industrial material used in plastic, paint, and other materials as a filler or additive, and has the advantage of being water resistant, high strength, high transparency, and non-toxic, making it ideal for biological applications. Since the glass microbubbles (average volumetric mass density = 0.6 g/cm^3, average diameter = 18 μm) have a much lower density than that of water, they can float on the surface of most liquids. A study has recently reported the use of the buoyancy of glass microbubbles for sorting CD4 positive T lymphocytes out from peripheral blood[8]. Interestingly, we found that when the microbubbles were entrapped within a water droplet, they would autonomously float to the top of the droplet and be concentrated into a dense circular monolayer, without the requirement of any external power source or devices. This self-concentrating characteristic of the hollow glass microbubbles allowed us to achieve an increased signal compared to similarly sized solid glass microbeads (Corpuscular) when both were coated with a fluorescent marker (fluorescent streptavidin-phycoerythrin, SAPE) using the same conjugation protocol and dispensed in a water droplet of same size (Fig. 1). We also noted that as the microbeads will sediment onto the substrate on the bottom of a droplet, it makes it much more difficult to accurately differentiate the background signal of the substrate from that

[a] Institute of Biomedical Engineering and Nanomedicine, National Health Research Institutes 35, Keyan Road, Zhunan Town, Miaoli County 35053, Taiwan.
[b] Department of Life Science, National Tsing Hua University, 101, Section 2, Kuang-Fu Road, Hsinchu 30013, Taiwan.

† Electronic Supplementary Information (ESI) available: Detailed materials and methods, and additional data. See DOI: 10.1039/x0xx00000x

of the signal from the microbeads (Fig. 1B, C), which is also evident in a previous report using glass microbeads packed in a microfluidic chamber for immunoassays[9]. Although this might not be a problem if the glass microbeads were only used for capturing antigens or cells from a heterogeneous sample[10] without the need for quantification, the differentiation of signal to background is crucial for high sensitivity quantitative immunoassays. On the other hand, as microbubbles float on the apex of the water droplet, far away from the substrate below, the focus plane of the microscope will also be much farther away from the substrate (Fig. 1A), the major source of the background signal, which translates to a lower background level.

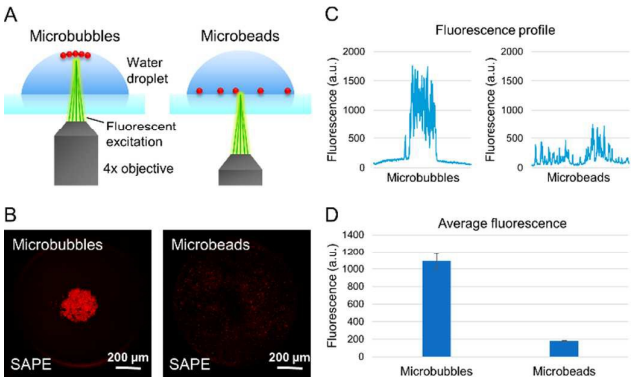

Fig. 1 Fluorescent signal intensity of buoyant hollow glass microbubbles vs. solid glass microbeads of similar size. (A) Schematic illustration of the microbubbles, which autonomously float and concentrate into a dense monolayer at the top of a water droplet, whereas microbeads randomly sediment at the bottom of the droplet. (B) Fluorescent images of fluorescent streptavidin-phycoerythrin (SAPE) conjugated microbubbles and microbeads inside a water droplet. (C) Quantified fluorescent intensity of a cross section of the fluorescent images in (B). (D) Average fluorescent intensity of microbubbles vs. microbeads. Error bars represent the standard deviation from 3 repeats.

We then proposed to take advantage of this self-concentrating characteristic of microbubbles to develop a high-sensitivity immunoassay, with the capability of multiplex screening (detection of multiple targets simultaneously from one sample). In multiplex immunoassays, different capture antibodies are conjugated onto different microparticles, then used to detect multiple targets simultaneously. Usually, microparticle based multiplex immunoassays require an identification "barcode" to identify the various different capture antibodies immobilized on different microparticles. Many particle identification codes have been developed for this reason, including optical[11], graphical[12], and electronic[13] encoding methods. The drawback to such encoding schemes is that they require sophisticated high-magnification optical or electronic equipment to decode the identity of the particles, and that the numbers of target molecules able to be simultaneously detected are limited by the number of codes available. Thus, in order to achieve a simpler and more robust operation without the requirement of a high-magnification lens, we proposed to design a microbubble based multiplex immunoassay platform that would not require particle encoding. One approach is to pattern the microbubbles in a spatially encoded microarray format like that in a planar microarray. Spatial encoding allows the identity of a capture antibody to be identified simply via its spatial location on a chip, thus eliminating the aforementioned complications from particle encoding and detection. This approach can allow for a much simpler and higher-throughput signal acquisition process while also providing the flexibility and sensitivity advantages of microbubbles.

To accomplish this goal, a trapping method would have to be developed in order to distribute microbubbles in a spatially encoded microarray format. A commonly used platform for manipulating particles is microfluidics, a field that involves the handling, transport, and analysis of small volumes of fluids inside micrometer-sized channels. Microfluidic devices can offer ways to retain, mix, and manipulate microparticles to improve the efficiency and signal detection sensitivity of immunoassays[1], while also reduce reagent/sample consumption and reaction time due to shorter diffusion distances[14]. However, no current method exists to discretely distribute different microparticles into their respective chambers in closed microfluidic systems. To our best knowledge, our proposed multiplex microparticle based immunoassays in a spatially encoded microarray format have not been previously demonstrated.

Here, tailoring to the buoyant characteristics of glass microbubbles, we designed a microfluidic device for generating droplet shaped liquid hemispheres for trapping microbubbles in a spatially encoded microarray format. The liquid hemispheres, apart from being able to trap microbubbles, also provides a dome shaped liquid convex to allow for microbubble concentration on the apex of the hemisphere. We designated this platform, consisting of capture antibody coated glass microbubbles trapped within a microfluidic liquid hemisphere array device for performing multiplex immunoassays, as the "microbubble array" (μBA), (Fig. 2).

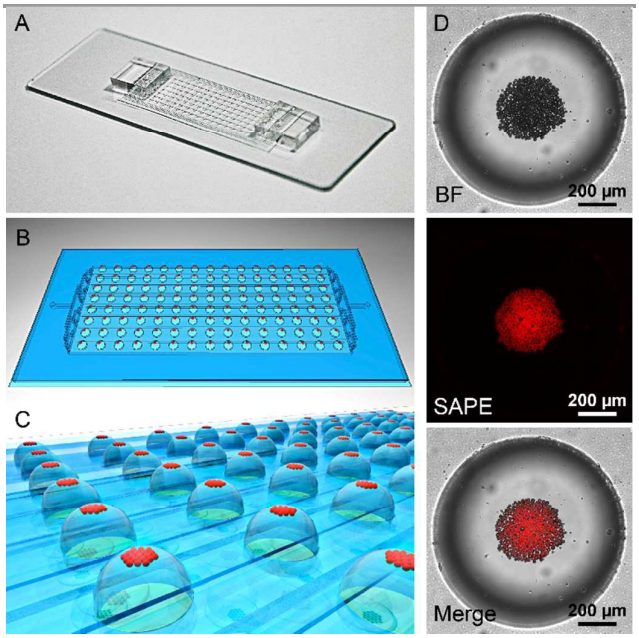

Fig. 2 Schematic of the μBA immunoassay platform. (A) Image of the microfluidic liquid hemisphere array device. Digitally rendered whole device (B), and close-up (C) image of the μBA platform, with microbubbles represented in red. (D) Microscope bright field (BF), fluorescent streptavidin-phycoerythrin (SAPE), and merged images of a single μBA liquid hemisphere with glass microbubbles trapped inside.

The microfluidic hemisphere array device was fabricated with polydimethylsiloxane (PDMS) using an open-air channel soft lithography technique[15], and consists of a total number of 120 circular openings (pores) with 1 mm diameter on top of a fluid channel. The pores are open to the air, thus after filling the device with solution, the circular pores can rapidly fill and form a liquid hemisphere on top of the pore (Fig. 2, 3A). The channel beneath the pores enable the batch exchange of analytes and wash solutions, thus allowing a parallel operation of the immunoassay.

Antibody conjugated glass microbubbles were prepared by first treating the microbubbles (iM30K, 3M corp.) with 1:1 (v/v) methanol in HCl for 30 minutes to hydroxylate the glass surface, followed by washing the microbubbles repeatedly in 99.8% ethanol, and finally silanizing the microbubbles with 10% (v/v) solution of 3-Aminopropyltriethoxysilane (APTES) in ethanol for 60 min. After washing the microbubbles again, they were incubated with 2.5% (v/v) Glutaraldehyde in PBS for 2 hours. Lastly, the microbubbles were incubated with capture antibody solution (anti-human TNF-α, anti-human IL-6), or 1% BSA (negative control) in PBS for 1 hour to covalently attach antibodies onto the glass surface.

Because glass microbubbles are 3-dimensional and optically transparent, they offer an obvious theoretical advantage in terms of signal enhancement because of (1) a much higher surface to volume ratio compared to 2-dimensional ELISA plates and microarrays, (2) signal localization due to the buoyancy of microbubbles, which simultaneously float and gather in a dense monolayer on the apex of the liquid hemisphere, and (3) due to a “lensing” and signal summation effect of the transparent spherical microbubbles. To confirm the signal amplifying effect of the glass microbubbles, we conjugated glass microbubbles and a conventional glass cover slip with fluorescent streptavidin-phycoerythrin (SAPE) and compared the fluorescent intensity of microbubbles to the cover slip. Our results showed that the glass microbubbles greatly enhanced the fluorescent signal intensity, displaying a signal amplifying effect of up to 22.7 times (arbitrary unit) compared to that of the cover slip (Fig. S1). The microbubbles also proved to be effective in serving as a lens for refracting light, which concentrates the fluorescent signal to a circular ring around the microbubbles when focused on the focal plane of the microscope (Fig. S2).

The μBA immunoassay was performed by the following steps. First, the microfluidic device was filled with 1% BSA in PBS to form the liquid hemisphere arrays (Fig. 3A). Then, capture antibody, and BSA conjugated microbubbles were spotted onto the liquid hemispheres using a needle (Fig. 3B). The sample containing the antigens of interest was flowed into the device with a syringe pump, to allow for antigens to attach to the capture antibodies on microbubbles (Fig. 3C). The microbubbles were then subsequently washed with PBST buffer to remove unbound antigens. Next, biotinylated detection antibody solution was flowed into the device to form a sandwich complex (Fig. 3D), washed with PBST, then incubated with fluorescent streptavidin-phycoerythrin (SAPE), which binds to the biotinylated detection antibodies (Fig. 3E). Lastly, the microbubbles were washed with PBST, and the fluorescent signal was scanned using an inverted microscope (Fig. 3F) equipped with an automated stage and epifluorescence.

The fluorescent signal of microbubbles were then quantified using an open-source software ImageJ (NIH). The fluorescent intensity was obtained by measuring the total pixel intensity in a circular selection divided by the area of the selection. For simplicity, the fluorescent intensity of microbubbles was measured on a region of tightly packed monolayer microbubbles on the apex of the liquid hemisphere, instead of measuring the individual microbubbles themselves.

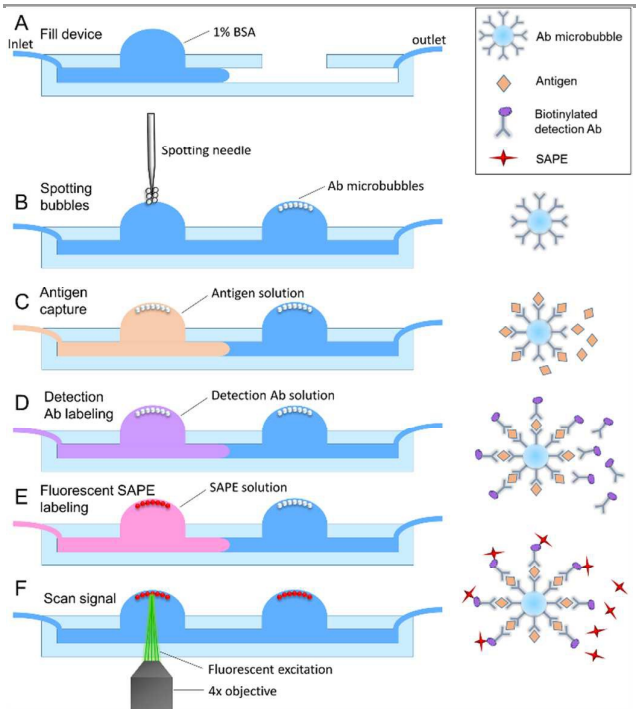

Fig. 3 Operation of the μBA immunoassay. The immunoassay was performed by (A) Filling the microfluidic device with 1% BSA to form the liquid hemisphere arrays. (B) Spotting Ab microbubbles onto the liquid hemispheres with the tip of a spotting needle. (C) Flowing the analyte solution into the device to allow antigens to attach to the Ab-microbubbles. (D) Flowing detection antibody solution into the device. (E) Flowing fluorescent SAPE solution into the device, and (F) scanning the fluorescent signal with a fluorescent microscope.

At the scale of microfluidic channels, most fluids display laminar flow, in which fluids flow in parallel layers with very little lateral movement, and mixing occurs only by diffusion. In addition, because diffusion time is proportional to the square of the diffusion length, a small increase in length would increase the required diffusion time a very significant amount. Thus, in order to enhance the solution mixing, binding kinetics and hence reduce the reaction time of the μBA immunoassay, we devised a sequential pumping method for delivering the samples and wash solutions (Fig. 4).

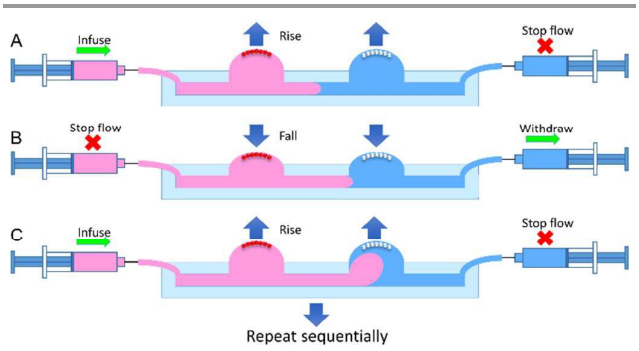

Fig. 4 Operation of the sequential pumping method. (A) For solution delivery, the solution was infused from the inlet while the flow out of the outlet was stopped. Thus all the infused solution would flow into the liquid hemisphere, increasing its size. (B) In the next step, the flow from the inlet was stopped, while the solution was being withdrawn from the outlet, exchanging the solution within the hemisphere. (c) The process was then repeated sequentially until all steps in the immunoassay were completed.

In brief, both the inlet and outlet of the device were connected to a syringe mounted on a syringe pump. For solution delivery, the solution was infused from the inlet at 20 μL/min for 20 s while the flow out of the outlet was stopped. In this way, no solution could exit the device, and all the infused solution would flow into the liquid hemisphere, increasing its size, and enhance mixing within the liquid (Fig. 4A). In the next step, the flow of the inlet was stopped, whereas the solution was actively withdrawn from the outlet at 20 μL/min, effectively exchanging the solution within the liquid hemisphere (Fig. 4B). The process was then repeated sequentially for 22 cycles (147μL of infused solution) for the antigen, detection antibody, and SAPE solutions, whereas the wash step (PBST) was repeated for 10 cycles, which we found to be sufficient for washing out the residual background signal in the device (67μL) (Fig. 4C).

To demonstrate that the μBA can successfully isolate microbubbles in different liquid hemispheres from each other, we spotted FITC (green) and ATTO 532 (red) fluorescent antibody conjugated glass microbubbles in alternating sequential order in the μBA (Fig. 5). After a sequential pumping operation like that in our immunoassay, we then scanned the device using green and red fluorescent filters. Results from the fluorescent overlay image showed that our μBA platform can isolate different microbubbles in a spatially encoded array format, without cross contamination occurring between each row and column of the array (Fig. 5).

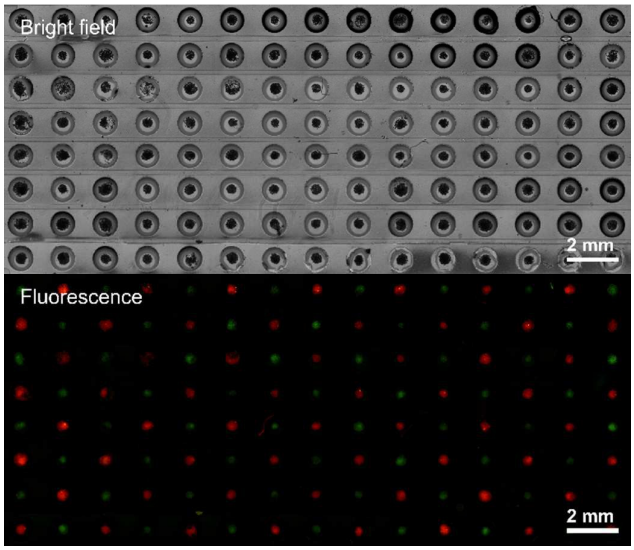

Fig. 5 Microbubble isolation ability of the microbubble array platform. FITC (green) and ATTO 532 (red) antibody conjugated glass microbubbles were spotted in alternating sequential order in the microbubble array platform. The fluorescent image showed that hardly any cross contamination occurred between each row and column of the array.

To test the multiplexing ability of our μBA platform, we spotted anti-human TNF-α, anti-human IL-6, and negative control (BSA) conjugated microbubbles in alternating rows on the liquid hemispheres (Fig. 6), and performed the multiplex

immunoassay using a pooled mixture of recombinant human TNF-α and human IL-6 as a model analyte. The results showed that the anti TNF-α and IL-6 conjugated microbubbles display a much brighter fluorescence than the BSA negative control microbubbles. (Fig. 6). We also validated that the antibodies used in our immunoassay are highly specific and exhibit no detectable cross reactivity with each other (Fig. S3). Note that because the microbubbles were suspended on the apex of the liquid hemisphere, far away from the microfluidic channel below, we observed very little background noise potentially generated from the nonspecific adsorption of analytes to the PDMS channel surface (Fig. 6). PDMS is known to have the tendency to easily adsorb biological molecules like proteins, thus generating unwanted background noise in previous microfluidic immunoassays due to non-specific adsorption[16]

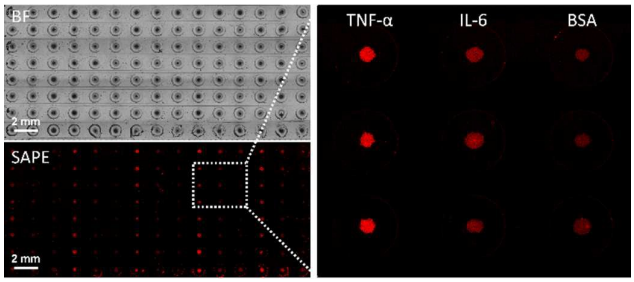

Fig. 6 Full image of the μBA platform after the immunoassay was completed. Glass microbubbles with different capture antibodies or negative controls were spotted in alternating rows on the liquid hemisphere array (from left to right: TNF-α, IL-6, BSA).

To evaluate the detection sensitivity and quantitative detection accuracy of the μBA platform, we performed the multiplex immunoassay with a pooled mixture of recombinant human TNF-α and human IL-6 serially diluted for 5 times with a 2 fold dilution ranging from 62.5 pg/mL to 1000 pg/mL for TNF-α, and 37.5 to 600 pg/mL for IL-6 respectively, then plotted the fluorescent signal intensity in respect to the solution concentration (Fig. 7). The limit of detection (LOD), defined as 3 times the standard deviation of the background signal, was found to be 7.46 pg/mL and 13.63 pg/mL for TNF-α and IL-6, respectively. On the other hand, using the same antibodies under the same conditions for a standard ELISA assay yielded lower sensitivities (LOD for TNF-α: 24.04 pg/mL; LOD for IL-6: 32.51 pg/mL) compared to our μBA platform (Fig. S4). We also confirmed that the fluorescent signal is indeed homogeneous throughout the device for both columns and rows, with a coefficient of variation (CV) of 12.95% (Fig. S5).
However, a potential disadvantage of our μBA platform is that it requires the precise manipulation of fluids with controlled flow rates using programmable syringe pumps, whereas current antibody microarray platforms do not have this requirement. Additionally, our current platform still relies on the traditional "sandwich" immunoassay method which requires the use of detection antibody labeling, whereas many reported label-free immunoassay platforms do not require labeling and hence can shorten and simplify the operational process of immunoassays. It would be of interest to integrate a label-free detection method like surface plasmon resonance (SPR) with our μBA platform in future studies.

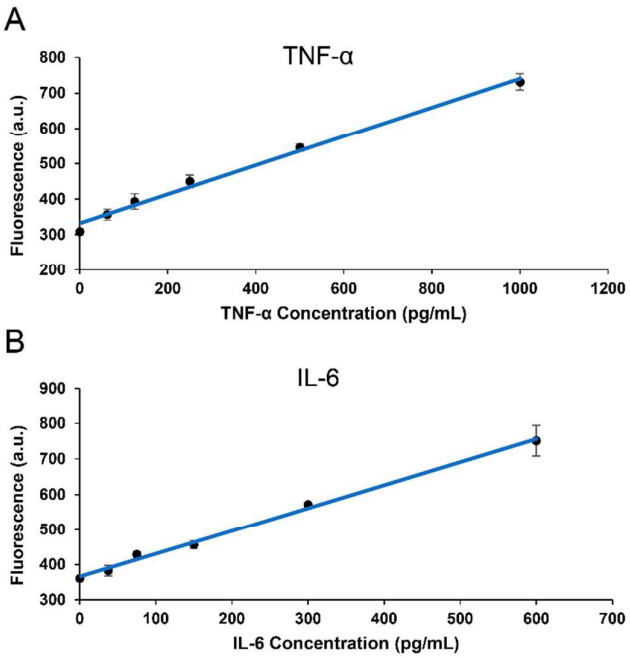

Fig. 7 Multiplex detection of human cytokines on the μBA platform. A pooled mixture of recombinant human TNF-α and human IL-6 were serially diluted for 5 times with a 2 fold dilution. (A) Calibration curves for TNF-α, and (B) IL-6 were then generated by quantifying the fluorescent intensity. The limit of detection for TNF-α and IL-6 are 7.46 pg/mL and 13.63 pg/mL, respectively.

Conclusions

To summarize, we have demonstrated a self-concentrating buoyant glass microbubble method for enhancing the sensitivity of immunoassays. The buoyancy of the glass microbubbles allow for autonomous concentration of an immunoassay signal, without the requirement of using an external device component for trapping the microbubbles. They are also 3-dimensional and transparent, which amplifies fluorescent signals for optical imaging. And lastly, we developed a μBA platform that allows microbubbles to be trapped in a spatially encoded microarray format for multiplex immunoassays. As the microbubbles float to the apex of the microfluidic liquid hemispheres, the background fluorescence generated by non-specific adsorption of analytes to the PDMS channel surface can be reduced. We also note that the open system design of our μBA platform allows the microbubbles to be retrieved individually after the assay, enabling the captured molecules to be potentially recovered for further downstream analyses. Alternatively, our platform may potentially be expanded to applications like high-throughput chromatin immunoprecipitation (HT-ChIP)[17].

Acknowledgements

We would like to thank the Ministry of Science and Technology (103-2815-C-400-001-E) for funding support, and 3M Corp. for providing the glass microbubbles as a gift.

Notes and references

1. S. Derveaux, B. G. Stubbe, K. Braeckmans, C. Roelant, K. Sato, J. Demeester and S. C. De Smedt, *Anal Bioanal Chem*, 2008, **391**, 2453-2467.
2. S. H. Kim, J. W. Shim and S. M. Yang, *Angew Chem Int Edit*, 2011, **50**, 1171-1174.
3. A. H. Diercks, A. Ozinsky, C. L. Hansen, J. M. Spotts, D. J. Rodriguez and A. Aderem, *Analytical biochemistry*, 2009, **386**, 30-35.
4. K. Sato, M. Tokeshi, T. Odake, H. Kimura, T. Ooi, M. Nakao and T. Kitamori, *Analytical chemistry*, 2000, **72**, 1144-1147.
5. J. Voldman, R. A. Braff, M. Toner, M. L. Gray and M. A. Schmidt, *Biophysical journal*, 2001, **80**, 531-541.
6. V. R. Daria, P. J. Rodrigo and J. Gluckstad, *Biosensors & bioelectronics*, 2004, **19**, 1439-1444.
7. H. Huang, X. L. Zheng, J. S. Zheng, J. Pan and X. Y. Pu, *Biomedical microdevices*, 2009, **11**, 213-216.
8. C. H. Hsu, C. Chen, D. Irimia and M. Toner, *Technology*, 2015, **3**, 38-44.
9. N. Y. Lee, Y. Yang, Y. S. Kim and S. Park, *B Kor Chem Soc*, 2006, **27**, 479-483.
10. Y. Wan, Y. L. Liu, P. B. Allen, W. Asghar, M. A. I. Mahmood, J. F. Tan, H. Duhon, Y. T. Kim, A. D. Ellington and S. M. Iqbal, *Lab on a chip*, 2012, **12**, 4693-4701.
11. N. H. Finkel, X. Lou, C. Wang and L. He, *Analytical chemistry*, 2004, **76**, 352A-359A.
12. D. C. Pregibon, M. Toner and P. S. Doyle, *Science*, 2007, **315**, 1393-1396.
13. W. Mandecki, B. Ardelt, T. Coradetti, H. Davidowitz, J. A. Flint, Z. L. Huang, W. M. Kopacka, X. Lin, Z. Y. Wang and Z. Darzynkiewicz, *Cytom Part A*, 2006, **69A**, 1097-1105.
14. A. H. Ng, U. Uddayasankar and A. R. Wheeler, *Anal Bioanal Chem*, 2010, **397**, 991-1007.
15. C. H. Hsu, C. Chen and A. Folch, *Lab on a chip*, 2004, **4**, 420-424.
16. M. W. Toepke and D. J. Beebe, *Lab on a chip*, 2006, **6**, 1484-1486.
17. R. Blecher-Gonen, Z. Barnett-Itzhaki, D. Jaitin, D. Amann-Zalcenstein, D. Lara-Astiaso and I. Amit, *Nature protocols*, 2013, **8**, 539-554.

